Aharonov-Bohm loops and multiprobe measurements

1995 J. Phys.: Condens. Matter 7 6675

(http://iopscience.iop.org/0953-8984/7/33/007)

J. Phys.: Condens. Matter 7 (1995) 6675–6685. Printed in the UK

Aharonov–Bohm loops and multiprobe measurements

Simon J Robinson
Department of Physics, University of Sheffield, Sheffield S3 7RH, UK

Received 10 April 1995, in final form 12 June 1995

Abstract. I study theoretically and numerically the conductance of a 1D mesoscopic ring in the localized regime, explicitly taking account of the four-probe nature of measurements. I show that a number of effects can arise that are absent from conventional theories of rings based on $G = (2e^2/h)T$: $h/2e$ and higher Fourier components appear even in the absence of electron trajectories that encircle the ring. The *sign* of the conductance can change periodically with the applied field, while the typical relative magnitude of the conductance oscillations may be highly sensitive to the arrangement of the probes. I also show that for samples sufficiently disordered the Aharonov–Bohm oscillations in the conventionally measured conductance vanish; a non-local conductance remains strongly flux sensitive.

1. Introduction

A consequence of the phase-coherent transport encountered in submicrometre devices in the so-called mesoscopic regime is the need to take into account the full geometry of the device, even in regions away from the classical current path [1–3]. Hence a full understanding of measured electrical conductances requires a formalism that explicitly takes into account the four-probe measuring techniques conventionally used. Several interesting effects that depend on multiprobe measurements have been observed, including the enhancement [4, 5] of the universal magnetoconductance fluctuations [6–8] when the voltage probe separations are smaller than a dephasing length and the negative bend conductance of crossed wires [9, 10], while the quantum Hall effect has also been related to multiprobe formulae [11, 12]. Recently it has been predicted that the longitudinal conductance of a superconducting wire may be negative even in the localized regime [13], and that the conductance of such a wire may reverse sign on switching on superconductivity or changing an applied magnetic field [14]. The purpose of this work is to highlight some further consequences of multiprobe measurements that appear for Aharonov–Bohm (AB) loops.

Although previous work on small rings has acknowledged that four-probe effects must be taken into account, consideration of this aspect has usually been confined to the observation that the conductance need not be symmetric with respect to sign reversal of the magnetic field because an off-diagonal Onsager coefficient is being measured [15, 16]. Beyond that, studies usually assume that the conductance is proportional to the transmission through the sample, $G = (2e^2/h)T$, which is correct for two-probe measurements [17], although DiVincenzo and Kane successfully used a multiprobe formalism to compute the typical magnitude of the AB oscillations in loops [18], while Ford *et al* have studied crossed wire systems including a system with a dot in the centre that has the topology of a ring [19]. Here I compute the longitudinal, bend, Hall and non-local conductances for a ring in the localized regime using the exact multiprobe expression derived in [1, 2]. I show that novel

0953-8984/95/336675+11$19.50

effects arise which are missed by calculations based on $G = (2e^2/h)T$: depending on the arrangements of the probes, the sign of the conductance can vary periodically with applied field; the relative magnitude of the oscillations as a ratio of the typical conductance for a given ring may be sensitive to which conductance is measured; and $h/2e$ and higher components may appear due to the complex nonlinear relationship between G and the various transmission coefficients in the system, even in the strongly localized case, for which contributions to transport from the weak localization effect [22] and transport paths that encircle the ring are negligibly small so that the two-probe conductance contains no higher components. A further consequence is that the conductance most sensitive to AB effects is not the longitudinal conductance G_L conventionally measured, but a non-local one, which can be strongly flux dependent even when G_L is effectively constant. In view of the complexity of the relationship between transport coefficients and multiprobe conductances, this work is confined to an analysis of single-channel wires at zero temperature and small applied voltages.

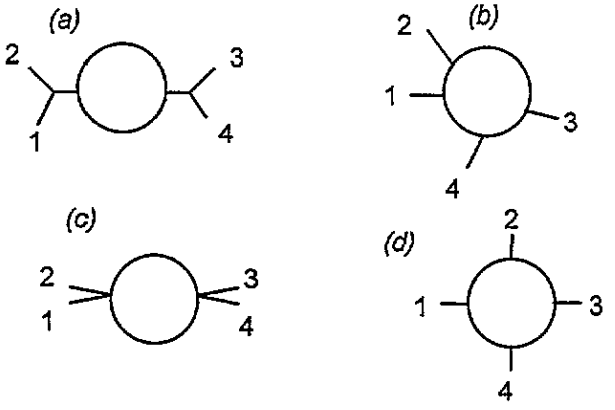

Figure 1. Different four-probe geometries: (a) the conventional experimental arrangement, (b) probes directly attached to ring, (c) probes directly attached and paired up, (d) probes directly attached and arranged at right angles around ring. The numbers label the probes.

The usual experimental arrangement for examining the Aharonov–Bohm effect in mesoscopic rings features two diametrically opposite connections (shown in figure 1(a)). A short distance away from the ring the connections each split into a current and a voltage probe [16]. Here I wish to address the question of what happens if the positions of the probes are varied. Accordingly I will examine rings such as that in figure 1(b), in which the current and voltage probes are directly attached to the ring. For our purposes the arrangement of figure 1(a) can be regarded as a special case of figure 1(b), for which the probes are paired up and diametrically opposite (figure 1(c)).

I will consider the case in which there is substantial localization along the ring, but the probes are clean. For this case the direct transmission amplitude along a path of length L_{mn} along the ring can be written as $t_{mn} = \exp(-L_{mn}/\xi_{mn}) \exp i\theta_{mn}$ where according to single-parameter scaling [20, for a recent review covering this area see 21] ξ_{mn} is taken from a Gaussian distribution with mean ξ and θ_{mn} is the phase associated with the path.

In general, for an AB loop, we expect $G(\Phi) = G_0 + \sum_{n=1,\ldots,\infty} \delta G_n \cos n(\Phi/\Phi_0 + \theta_n)$, with a similar expression for the resistance R, where Φ is the flux through the ring, Φ_0 is the flux quantum h/e and the θ_n are phase angles that are chosen to ensure all the δG_n are positive. Terms for successively higher values of n involve paths in which the

electrons encircle the ring multiple times. Hence in the localized regime these terms decay exponentially with n, and only the first terms G_0 and δG_1 are significant. I will develop a theory based on the typical behaviour of the relative magnitude of the fluctuations, irrespective of the phase. This implies considering ensemble-averaged components of the conductances. It should be noted however that this is distinct from the averaging procedure commonly employed, in which $\langle G(\Phi)\rangle$ is directly computed as a function of Φ: for that case, all components with odd n average to zero, whilst those with even n do not due to weak localization effects [23–29]. Hence, even if δG_1 dominates for a single sample, this is not the case after averaging. However, since we are studying the *magnitudes* of the respective Fourier components, such averaging to zero does not take place and it is therefore correct to consider only the h/e oscillations in the transmission probabilities. Subsequent computer simulations will examine how the conductances behave in practice for individual samples.

2. Theory

We may obtain the flux dependence of the transmission amplitude by writing it as a Feynmann sum over paths. This method of analysis has been used to describe wire networks in [31–33]. Since we are interested in the localized limit we ignore contributions from long paths encircling the ring, and since we will be interested only in the orders of magnitudes of the contributions from different trajectories, we neglect the numerical factors introduced by scattering at the nodes. As an example consider the transmission amplitude t_{21} from probe 1 to probe 2 of figure 1(b). We use subscripts γ_1 and γ_2 to respectively label the upper and lower paths round the ring, and on summing over direct paths deduce

$$t_{21} = \exp(-L_{\gamma 1}/\xi_{\gamma 1}) \exp \mathrm{i}\theta_{\gamma 1} \exp\left(\frac{\mathrm{i}h}{e}\int_{\gamma 1} \boldsymbol{A}\cdot \mathrm{d}\boldsymbol{l}\right) + \exp\left(-L_{\gamma 2}/\xi_{\gamma 2}\right) \exp \mathrm{i}\theta_{\gamma 2} \exp\left(\frac{\mathrm{i}h}{e}\int_{\gamma 2} \boldsymbol{A}\cdot \mathrm{d}\boldsymbol{l}\right) \tag{1}$$

where $\boldsymbol{A}$ is the magnetic potential corresponding to a flux Φ threading the ring. Hence

$$T = |t_{21}|^2 = \exp\left(-2L_{\gamma 1}/\xi_{\gamma 1}\right) + \exp(-2L_{\gamma 2}/\xi_{\gamma 2}) + 2\exp(-L_{\gamma 1}/\xi_{\gamma 1} - L_{\gamma 2}/\xi_{\gamma 2}) \cos(\theta_{\gamma 1} - \theta_{\gamma 2} + \Phi/\Phi_0). \tag{2}$$

This expresses the intuitive result that the typical magnitude of the transmission probability is essentially determined by the individual path having the largest transmission amplitude, while the Aharonov–Bohm oscillations are of the order of the product of the transmission probabilities around each arm of the ring. A consequence of this formula is that the AB effect is most apparent when both arms have transmission amplitudes of roughly equal magnitude. This can be seen if we assume that $L_{\gamma 1}/\xi_{\gamma 1} < L_{\gamma 2}/\xi_{\gamma 2}$, so that the second term in (2) may be neglected, and

$$T \approx \exp(-2L_{\gamma 1}/\xi_{\gamma 1})\left[1 + 2\exp\left(-\left(L_{\gamma 2}/\xi_{\gamma 2} - L_{\gamma 1}/\xi_{\gamma 1}\right)\right) \cos(\theta_{\gamma 1} - \theta_{\gamma 2} + \Phi/\Phi_0)\right]. \tag{3}$$

Hence the relative conductance fluctuation $\delta G_1/G_0$ is of order $\exp(-(L_{\gamma 2}/\xi_{\gamma 2} - L_{\gamma 1}/\xi_{\gamma 1}))$.

In general the different ξ_j for different segments of the ring will be independent random numbers taken from a normal distribution. Although *on average* the transmission amplitudes

will decay exponentially with path length it is quite possible for a longer path to have a higher amplitude than a shorter one. However, taking into account the full distribution of the ξ in the multiprobe conductance formulae would severely complicate the theory. Since our aim is to develop a tractable theory that may be used to develop a physical understanding of multiprobe measurements on rings, we will assume instead that it is possible to approximately replace the ξ_j by a single value ξ. While this appears unrealistic, subsequent computer simulations will show that it does give a useful first approximation. We also note that our model does correctly describe the case for which localization results from tunnelling through a potential barrier without disorder.

We consider first the longitudinal conductance G_L of the ring. In the localized limit this result would be expected to give similar results to a two-probe measurement [2, 13]. To show this explicitly, we consider figure 1(c) and define the four-probe conductance $G_L = G_{jklm} = I_j/V_l - V_m$ subject to $I_k = -I_j$, $I_l = I_m = 0$, where I_j is the current flowing into the device from probe j and V_j is the potential on reservoir j. This quantity was shown by Büttiker [1, 2] to be given by the expression

$$G_{jk,lm} = D/(T_{lj}T_{mk} - T_{mj}T_{lk}) \tag{4}$$

where the quantity D is independent of which probes are chosen to supply the current and is given by [13]

$$\begin{aligned} D = {} & T_{12}T_{23}T_{34} + T_{12}T_{24}T_{34} + T_{13}T_{21}T_{34} + T_{14}T_{21}T_{34} \\ & + T_{12}T_{24}T_{31} + T_{12}T_{24}T_{32} + T_{34}T_{13}T_{23} + T_{34}T_{13}T_{24} \\ & + T_{21}T_{14}T_{31} + T_{21}T_{14}T_{32} + T_{34}T_{14}T_{23} + T_{34}T_{14}T_{24} \\ & + T_{13}T_{24}T_{32} + T_{14}T_{23}T_{31} + T_{14}T_{24}T_{31} + T_{14}T_{24}T_{32}. \end{aligned} \tag{5}$$

We now note that for the arrangement of figure 1(c) the transmission probabilities in (5) can be divided into two types. Those involving transmission between probes on opposite sides of the ring, e.g. T_{13} and T_{24}, have the form

$$T_{jk} = \exp(-L/\xi)\left(a_{jk} + b_{jk}\cos\left(\frac{\Phi}{\Phi_0} + \theta_{jk}\right)\right) \tag{6}$$

where L is the total circumference of the ring, a_{jk} and b_{jk} are real positive constants of order unity which take account of any slight asymmetries between the quadrants of the ring, and θ_{jk} is a phase angle. By contrast, transmission coefficients between adjacent probes have the form

$$T_{jk} = a'_{jk} + b'_{jk}\cos\left(\frac{\Phi}{\Phi_0} + \theta'_{jk}\right)\exp(-L/\xi). \tag{7}$$

We will also consider transmission between probes situated at right angles around the ring, for example probes 1 and 4 in figure 1(d). This yields the form

$$T_{jk} = \exp(-L/2\xi)[a''_{jk} + b''_{jk}\cos\left(\frac{\Phi}{\Phi_0} + \theta''_{jk}\right)\exp(-L/2\xi)]. \tag{8}$$

Since we are interested in the relative orders of magnitude of the typical conductance and of the Aharonov–Bohm oscillations we need to find the respective field-independent term and field-dependent term in G of the highest magnitudes. We use the generic symbols $\mathcal{A}$, $\mathcal{O}$ and $\mathcal{R}$ to represent transmission probabilities between adjacent probes, diametrically opposite probes and probes situated at 90° respectively. Now D is the sum of 16 terms, of which four are of the form $\mathcal{AAO}$, eight are of the form $\mathcal{AOO}$ and four are of the form $\mathcal{OOO}$. The largest field-independent contributions come from the $\mathcal{AAO}$ terms and are of

order $\exp(-L/\xi)$, as do the largest field-dependent contributions. Terms in $\cos^2(\Phi/\Phi_0)$ are exponentially smaller. For the conventional experimental arrangement, the quantity measured $G_L = G_{13,24}$, hence the denominator becomes $T_{21}T_{43} - T_{41}T_{23}$, which is of the form $\mathcal{AA} - \mathcal{OO}$. This has largest field-independent and field-dependent terms of respective orders unity and $\exp(-L/\xi)$. We deduce that

$$G_{13,24} \sim \frac{c_1 \exp(-L/\xi) + c_2 \exp(-L/\xi)\cos(\Phi/\Phi_0 + \theta_1)}{c_3 + c_4 \exp(-L/\xi)\cos(\Phi/\Phi_0 + \theta_2)}$$
$$\sim \exp(-L/\xi)\,[c_5 + c_6 \cos(\Phi/\Phi_0 + \theta_1)] \tag{9}$$

where the c_j are constants of order unity. We may now apply the above reasoning to different arrangements of the probes. We consider first the situation of figure 1(c), but for which the conductance measured is the non-local conductance $G_N = G_{12,34}$. Then D is unchanged, but the denominator becomes $T_{31}T_{42} - T_{41}T_{32}$, which is of the form $\mathcal{OO} - \mathcal{OO}$. Since both terms are of equal magnitude, the result may be positive or negative. Assuming that the denominator is non-zero, which will essentially always be true due to asymmetries, we find

$$G_{12,34} \sim \pm \exp(L/\xi)\,\frac{c_1 + c_2 \cos(\Phi/\Phi_0 + \theta_1)}{c_7 + c_8 \cos(\Phi/\Phi_0 + \theta_3)}. \tag{10}$$

This expression is not a simple sinusoidal form, and implies that even if G_N never diverges, it will contain higher $h/2e$ and higher-frequency components. We stress that our model explicitly excludes all weak-localization contributions to the transmission coefficients and that therefore the existence of these higher components is due entirely to the nonlinear relation contained in (5). We also note that the non-local conductance increases with disorder because an exponentially large current must flow in the current probes in order to exactly cancel any current supplied from the voltage reservoirs.

Now we consider the arrangement of figure 1(d), for which the probes are arranged at right angles around the ring. Here D is sum of 16 terms, of which four are of the form $\mathcal{RRR}$, eight are of the form $\mathcal{RRO}$ and four are of the form $\mathcal{ROO}$. The largest field-independent terms come from the $\mathcal{RRR}$ terms and are of order $\exp -3L/2\xi$, while the highest field-dependent terms originate from the $\mathcal{RRR}$ and $\mathcal{RRO}$ terms and are of order $\exp -2L/\xi$. We are interested in the order of magnitude of the bend conductance $G_B = G_{12,43}$ and the Hall conductance $G_H = G_{13,24}$. For the bend conductance, the denominator is of the form $\mathcal{RR} - \mathcal{OO}$, so that

$$G_{12,43} \sim \exp(-L/2\xi)\left[c_9 + c_{10} \exp(-L/2\xi)\cos(\Phi/\Phi_0 + \theta_4)\right]. \tag{11}$$

We note that the AB oscillations are of the same order of magnitude as for the usual longitudinal arrangement, but that they are now swamped by the much larger mean conductance. On the other hand, for the Hall conductance the denominator is of the form $\mathcal{RR} - \mathcal{RR}$, so that the conductance may be of either sign. Assuming the terms in the denominator do not exactly cancel, we obtain

$$G_{13,24} \sim \pm \exp(-L/2\xi)\left[c_{11} + c_{12} \exp(-L/2\xi)\cos(\Phi/\Phi_0 + \theta_5)\right]. \tag{12}$$

For the Hall and non-local conductances, the question immediately arises of whether the sign of G for a given sample is fixed or whether it can be changed by changing the flux through the loop. We now present the results of computer simulations that show that the sign can in fact vary with applied flux.

3. Simulations

In order to test how the above order of magnitude calculations apply in practice, we performed simulations of disordered rings. The disorder was introduced via a piecewise constant potential around the loop: the total loop circumference was taken as $4 \times 10^4/k_F$, (k_F = inverse Fermi wavevector) and was divided into 400 cells of equal length. Within each cell the potential (relative to the Fermi energy E_F) was chosen randomly from a uniform distribution centred on zero and of width $2V$ (V measured in terms of E_F), with $V = 0.9$. The transmission probabilities between the various probes were calculated using the S matrix reduction algorithm described in [33]. This algorithm yields the exact transmission probabilities including all possible contributing paths. In all cases, the plots shown are the first 10 produced on the computer, but further simulation results were checked to ensure the presented plots were typical.

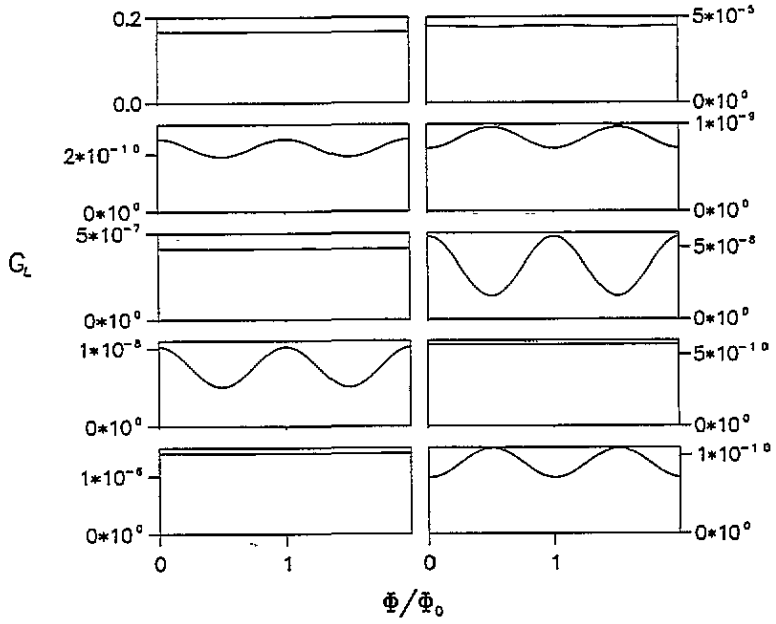

Figure 2. Typical plots of the longitudinal conductance for 10 different realizations of disorder with $V = 0.9$.

Figure 2 shows 10 plots of the G_L, varying over two cycles of flux (zero to $2h/e$), and confirms that G_L behaves essentially as the the two-probe conductance. In particular, the curves are sine waves with no evidence of higher-frequency components. Figure 3 presents the non-local conductances of the same samples, and we see immediately that sign changes not only do occur, but are extremely common. Only two out of the 10 results shown failed to reverse sign and both show higher-frequency components (the plots are not sine waves). The sign changes occur via a singularity in G because it is the denominator of (5) that can vanish due to cancellations. Bend and Hall conductances for new samples are shown in figures 4 and 5. We note that the Hall conductance reverses sign, though not nearly as often as the G_N. Where sign changes do not occur, the AB oscillations are often very weak in agreement with (12). On the other hand, G_B behaves very differently from the prediction of (11): although usually positive, it can reverse—actually doing so more readily than G_H

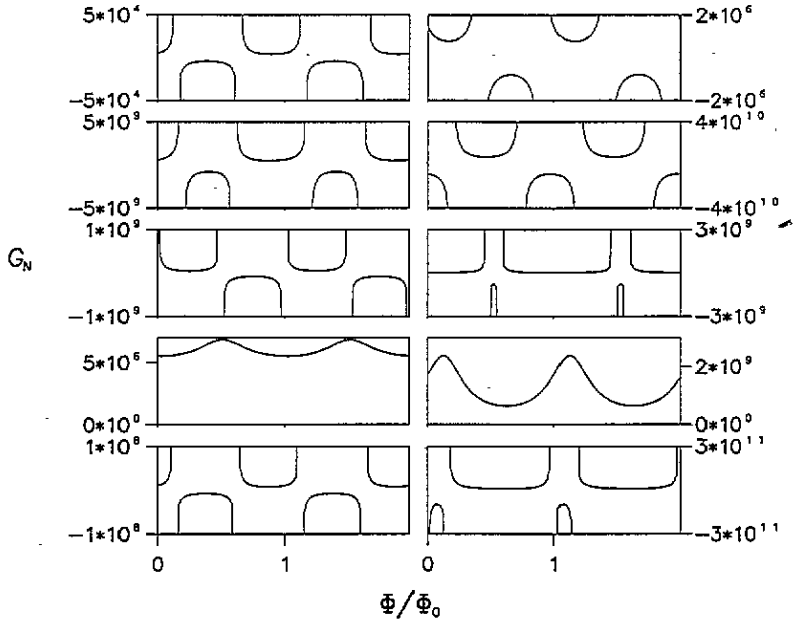

Figure 3. Plots of the non-local conductance for the same realizations of disorder as for figure 2.

for the systems studied, although it is not clear whether this is simply a statistical fluke. The AB oscillations are suppressed slightly in comparison to G_L—this is more apparent in

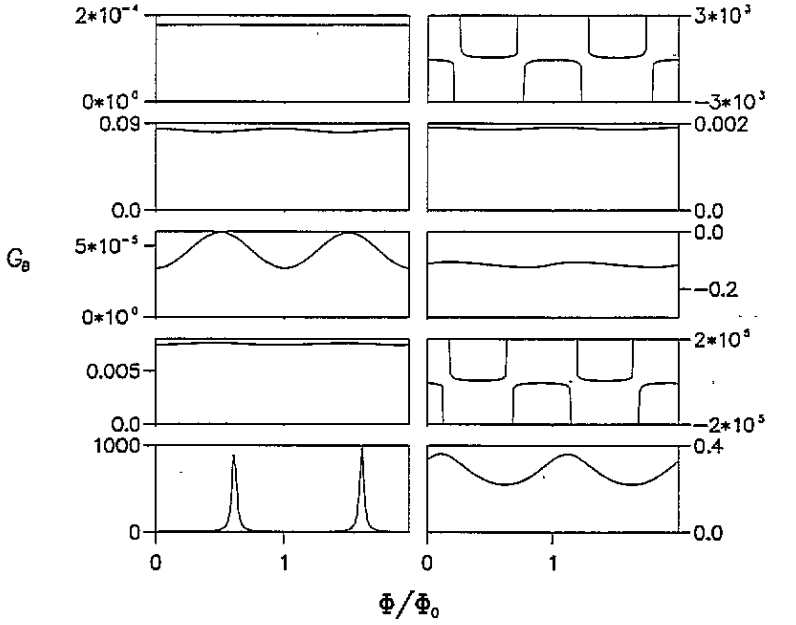

Figure 4. Typical plots of the bend conductance for 10 different realizations of disorder with $V = 0.9$. (NB these are different samples from those of figures 2 and 3.)

figures 6 and 7, in which the longitudinal and bend conductances are plotted for the higher disorder $V = 1.0$. The figures also clearly show how much more sensitive the non-local (and occasionally the bend and Hall) conductance is than G_L to the flux: several of the plots in figures 2 and 6 show no discernible oscillations while the corresponding G_N fluctuate strongly. The G_N for $V = 1$ are not shown, but behave similarly to those of figure 3.

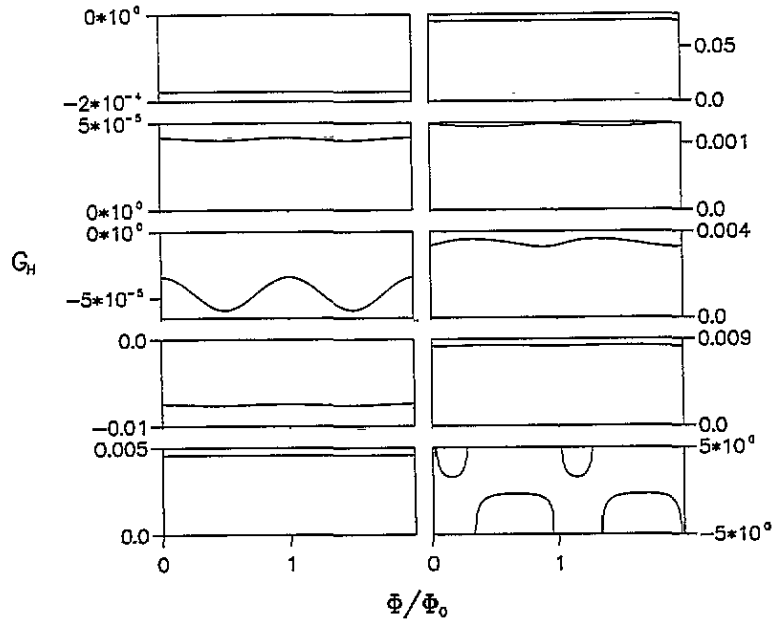

Figure 5. Plots of the Hall conductance for the same realizations of disorder as for figure 4.

To understand why our order of magnitude theory fails in these cases we need to allow for the effects of the localization length varying. We consider first G_B, which has a denominator of the form $\mathcal{RR} - \mathcal{OO}$. Now although the $\mathcal{R}$ transmission probabilities are typically exponentially smaller than the $\mathcal{O}$ ones,this is not always the case. If we assume that each log T has a normal distribution with mean value and variance of the same order of magnitude, and that the mean of the distribution for $\mathcal{O}$-type transmission probabilities is twice that for $\mathcal{R}$-type probabilities, we immediately see that there is a finite chance of the $\mathcal{RR}$ and $\mathcal{OO}$ terms being of the same order of magnitude, so that cancellations and near cancellations in the denominator can occur. This explains the simulated behaviour of G_B. On the other hand, G_L has an $\mathcal{AA} - \mathcal{OO}$ denominator. The $\mathcal{A}$-type transmission probabilities will have magnitude $\sim$ unity, so that they will almost always be greater than the $\mathcal{O}$ terms, and hence (9) accurately describes G_L.

To explain why G_N is more susceptible to sign changes than G_H although both have similar symmetries, we note that for G_H, due to the differing localization lengths for different segments of the ring, in practice one of the $\mathcal{RR}$ terms in the denominator of (4) will usually be larger than the other by at least an order of magnitude. However, expression (2) shows that the individual T_{ij} vary only weakly with Φ. Hence one of the $\mathcal{OO}$ terms remains the dominant one throughout the range of Φ and the majority of samples do not show sign changes, although G_H is equally likely to be positive for all Φ or negative for all Φ. On the other hand, the denominator of G_N is $T_{31}T_{42} - T_{41}T_{32}$. Now since probes 1 and 2 are adjacent, we have that $T_{31} \approx T_{32}$ and $T_{41} \approx T_{42}$, so that the two terms are of roughly

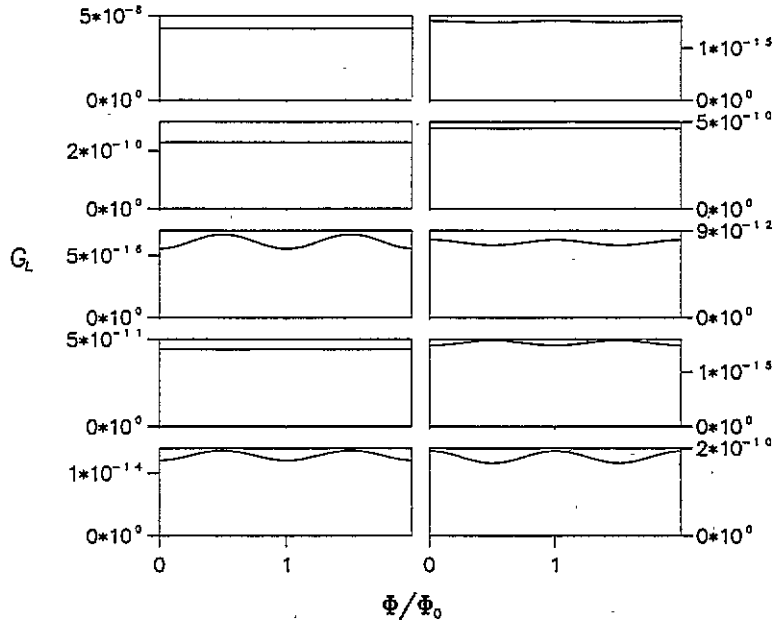

Figure 6. As figure 2, but for $V = 1.0$.

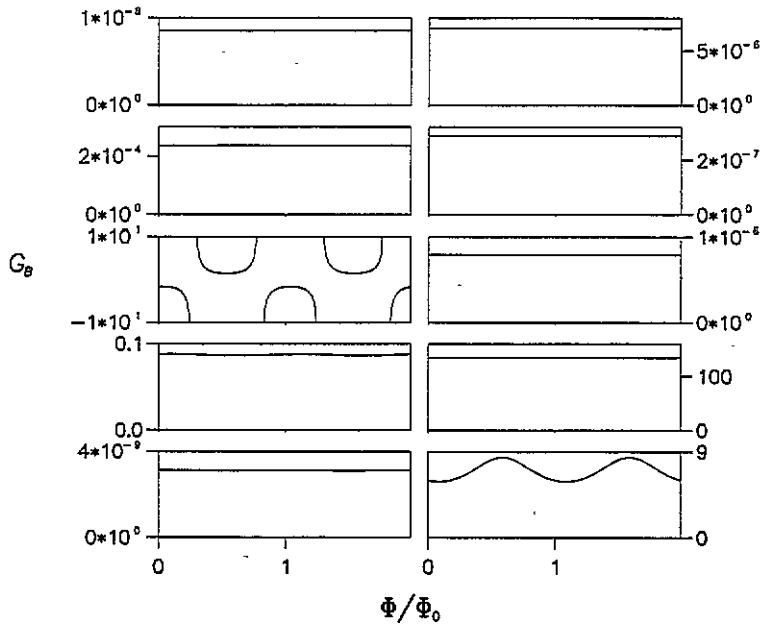

Figure 7. As figure 4, but for $V = 1.0$.

equal magnitude. Hence sign changes occur much more readily as Φ is varied. The above reasoning was confirmed by examining the individual T_{ij} calculated during the simulations.

4. Discussion

We have shown how it is possible to obtain a qualitative understanding of the various multiprobe conductances of an AB ring by considering the orders of magnitudes of the various terms in terms in the Büttiker four-probe conductance formula for this system, and have predicted several effects that arise from the four-probe nature of the measurements. We have shown that of the situations considered the conductance most sensitive to the flux through the ring is not the longitudinal conductance conventionally measured, but the non-local conductance. Apart from the longitudinal conductance, all the conductances considered can change sign with the flux through the ring, and even when this does not happen, $h/2e$ and higher components can be introduced although they may be absent from the corresponding two-probe measurements.

This work is not the first to point out sign changes in multiprobe conductances: these have been observed in wires coupled by a ballistic window [34] and predicted for the longitudinal conductance of disordered superconducting wires [14]. The novelty of the sign changes noted here is that they occur in normal wires in the localized limit, and are periodic with the flux.

Finally, we comment on how our results might apply to multichannel rings with a large aspect ratio. For such rings, (5) applies, however each T_{ij} is now not a simple transmission coefficient, but a sum of all transmission probabilities between probes i and j. Where the number of channels is relatively small, the h/e oscillations will continue to dominate over the $h/2e$ components in the localized limit, and we might expect the results of this paper to remain valid. On the other hand, in the limit of a large number of channels, the h/e oscillations and all odd harmonics will disappear from the T_{ij} due to averaging effects, so that $G_{ij,lm}$ is periodic with period $h/2e$, and the behaviour of the four-probe conductances is less clear. Similar effects will occur as the temperature is raised [27, 28]. It seems possible that in this case, G_N, G_H and G_B may continue to reverse sign periodically, now with period $h/2e$, but further work is clearly needed to clarify this.

Acknowledgments

This work has benefited from useful discussions with Colin Lambert and email correspondence with Keith Slevin and Angus MacKinnon. The simulations were performed on a program supplied by Mark Jeffery. Financial support from the EPSRC is also acknowledged.

References

[1] Büttiker M 1986 *Phys. Rev Lett.* **57** 1761
[2] Büttiker M 1988 *IBM J. Res. Dev.* **32** 317
[3] Umbach C P, Santhanam P, van Haesendonck C and Webb R A 1987 *Appl. Phys. Lett.* **50** 1289
[4] Skocpol W J, Mankiewich P, Howard R E, Jackal L D, Tennant D M and Stone A D 1986 *Phys. Rev. Lett.* **56** 2865
[5] Skocpol W J, Mankiewich P, Howard R E, Jackal L D, Tennant D M and Stone A D 1987 *Phys. Rev. Lett.* **58** 2347
[6] Webb R A, Washburn S, Umbach C P and Laibowitz R B 1985 *Phys. Rev. Lett.* **54** 2696
[7] Lee P A and Stone A D 1985 *Phys. Rev. Lett.* **55** 1622
[8] Lee P A, Stone A D and Fukuyama H 1987 *Phys. Rev.* B **35** 1039
[9] Avishai Y and Band Y B 1989 *Phys. Rev. Lett.* **62** 2527
[10] Y Takagaki, K Gamo, Namba S, Ishida S, Takaoka S, Murase K, Ishibashi K and Aoyagi Y 1988 *Solid State Commun.* **68** 1051

[11] Büttiker M 1988 *Phys. Rev.* B **38** 9375
[12] Büttiker M 1992 *The Quantum Hall Effect in Open Conductors, in Semiconductors and Semimetals* vol 35 (New York: Academic)
[13] Robinson S J, Lambert C J and Jeffery M 1994 *Phys. Rev.* B **50** 9611
[14] Allsopp N K, Hui V C, Lambert C J and Robinson S J 1994 *J. Phys.: Condens. Matter* **6** 10475
[15] Benoit A D, Washburn S, Umbach C P, Laibowitz R B and Webb R A 1986 *Phys. Rev. Lett.* **57** 1765
[16] Good reviews of experiments and theoretical work on AB rings, and detailed references, are contained in
Washburn S and Webb R A 1986 *Adv. Phys.* **35** 375
and more recently in
Washburn S 1991 *Mesoscopic Phenomena in Solids* ed B L Al'tshuler, P A Lee and R A Webb (Amsterdam: Elsevier)
[17] Büttiker M, Imry Y, Landauer R and Pinhas S 1985 *Phys. Rev.* B **31** 6207
[18] DiVincenzo D P and Kane C L 1988 *Phys. Rev.* B **35** 3006
[19] Ford C J B, Washburn S, Büttiker M, Knoedler C M and Hong J M 1990 *Surf. Sci.* **229** 298
[20] Thouless D J 1973 *Phys. Rep.* **13** 93
[21] Kramer B and MacKinnon A 1993 *Rep. Prog. Phys.* **56** 1469
[22] Bergmann G 1984 *Phys. Rep.* **107** 1
[23] Al'tshuler B L, Aronov A G and Spivak B Z 1981 *JETP Lett.* **33** 95
[24] D'amato J L, Pastawski H M and Weisz J F 1989 *Phys. Rev.* B **39** 3554
[25] Frahm K and Mühlschlegel B 1994 *Z. Phys.* B **94** 201
[26] Li Q and Soukoulis C M 1986 *Phys. Rev. Lett.* **57** 3105
[27] Stone A D and Imry Y 1986 *Phys. Rev. Lett.* **56** 189
[28] Murat M, Gefen Y and Imry Y 1986 *Phys. Rev.* B **34** 659
[29] Vasilopoulos P and Van Vliet C M 1993 *Solid State Commun.* **61** 121.
[30] Jeffery M, Green C, Tyagi S and Gilmore R 1989 *Phys. Rev.* B **39** 9054
[31] Jeffery M and Gilmore R 1990 *Phys. Rev.* B **41** 2057
[32] Robinson S J and Jeffery M 1995 *Phys. Rev.* B at press
[33] Hirayama Y, Wieck A D, Bever T, von Klitzing K and Ploog K 1992 *Phys. Rev.* B **46** 4035